



Sarafianou, M., Preece, A. W., Craddock, I. J., Klemm, M., & Leendertz, J. (2016). Evaluation of Two Approaches for Breast Surface Measurement Applied to a Radar-Based Imaging System. *IEEE Transactions on Antennas and Propagation*, 64(2), 609-617. DOI: 10.1109/TAP.2015.2499758

Peer reviewed version

Link to published version (if available):
[10.1109/TAP.2015.2499758](https://doi.org/10.1109/TAP.2015.2499758)

[Link to publication record in Explore Bristol Research](#)
PDF-document

This is the author accepted manuscript (AAM). The final published version (version of record) is available online via IEEE at <http://ieeexplore.ieee.org/xpl/articleDetails.jsp?reload=true&arnumber=7327159>. Please refer to any applicable terms of use of the publisher.

University of Bristol - Explore Bristol Research

General rights

This document is made available in accordance with publisher policies. Please cite only the published version using the reference above. Full terms of use are available:
<http://www.bristol.ac.uk/pure/about/ebr-terms.html>

Evaluation of Two Approaches for Breast Surface Measurement applied to a Radar-based Imaging System

Mantalena Sarafianou, A.W. Preece, I. J. Craddock, M. Klemm, J. A. Leendertz

Abstract— Locating the surface of an object, in this case the breast, is an important first step in many imaging situations; this surface information may be a necessary part of the reconstruction, it may be needed for the cancellation of the surface reflection, or (as herein) it may be needed as a preparatory step before imaging.

This paper presents two complementary approaches developed for the purpose of surface localisation. The proposed approaches are evaluated using data from both phantom measurements and volunteer scans.

Index Terms - Breast cancer detection, radar-based microwave imaging, breast surface reconstruction, surface identification.

I. INTRODUCTION

Breast cancer is the most common cancer in women worldwide [1, 2]. The ability of X-ray mammography to detect cancer at an early stage and reduce the mortality rates has resulted in it having a secured place in routine health checks and screenings for women [1, 2]. Despite its success, it also has significant limitations and risks (e.g. false-positives and false-negatives, health concerns regarding the exposure to ionising radiation, poor suitability for younger women with higher breast tissue density etc.) [1, 3]. This has prompted the development of alternative microwave methods which can contribute towards cancer diagnosis [4].

Three major approaches to microwave breast imaging have been thoroughly investigated in the previous decades, namely active, passive and hybrid [4, 5]. One category of active microwave techniques is classified as “*radar-based*” [4]. In this category, an image is constructed based on microwave energy reflections from dielectric scatters in the breast (i.e. possible tumours, inhomogeneous breast tissues) and reflections at the breast-skin interface [4].

In 2010, the University of Bristol developed a 31-element multi-static radar system for early stage breast cancer detection [6]. In 2011, the latest imaging system for breast cancer detection consisting of 60 antenna elements was presented [7, 8].

In both imaging systems, the patient lies in a prone position with the breast placed in a matching Eccostock ceramic cup ($\epsilon_r=9.5$ at 6GHz) with low losses [6-9]. In order to accommodate patients with different breast sizes, several ceramic inserts of the same material and properties were designed, which can be fitted into the main ceramic cup [7, 8].

In between all the various interfaces (i.e. ceramic cup and array, ceramic cup and insert) a small amount of a matching medium ($\epsilon_r=9$ and 1.2dB of attenuation at 6GHz) is used [6-9]. Prior to positioning the patient’s breast in the cup/ insert, a small amount of the same medium is used in order to ensure maximum contact between the breast and the shell and avoid air gaps [6-9].

Before image focusing [9, 10], the undesired skin reflection signal contributions are removed from the radar signals. This is achieved by forming the difference between two data sets obtained from the measurement of a patient’s breast in two positions by manually rotating the antenna array [6-10]. The differential signals obtained in this fashion for every possible bistatic pair of antennas are then focused by a Delay-and-Sum (DAS) algorithm [9, 10].

Reconstructing the surface of the breast, which is useful information in any such imaging system, is important for this particular system because in a clinical situation, the size of the patient’s breast may not exactly match that of any of the available ceramic inserts. Once a small amount of matching medium is applied in the insert and the breast is placed in the ceramic insert, air or excess fluid can be trapped between the insert and the patient’s breast. This situation is a bad fit. On the contrary, for a good match between the patient’s breast and the ceramic insert, the air is pushed out of the insert by the matching medium as the breast is placed in the insert. This is a good fit.

For the case of a bad fit, the radar signals will contain reflections due to the matching medium-air and air-skin interfaces. On rotating the array, the position of the badly-fitted area will be slightly shifted. After the subtraction of the two data sets, the majority of the skin reflection signal contributions will be cancelled. However, there will be skin reflection residuals due to the badly fitted area (i.e. gap) that during image focusing will result in clutter and artifacts.

The 60-element array can detect 7mm diameter tumour phantoms [10] in a homogeneous breast phantom with the dielectric contrast between the tumour and normal tissue being 2:1. Based on clinical experience and as discussed in the previous paragraph; a gap of a few millimetres could result in

the introduction of clutter in the imaging result and thus the inaccurate detection of the tumour. Hence, it is desirable for the patient's breast to be properly-fitted into the ceramic cup prior to taking a measurement. The quality of the breast fitting could be determined through the estimation of the breast surface relatively to the ceramic cup/ insert used. Since the patient is in prone position and the array is fully populated it is impossible to visually determine whether the patient's breast is in fact properly-fitted. Thus, a full breast surface reconstruction will be necessary.

Several breast surface reconstruction algorithms have been developed by various research groups to be used by microwave imaging prototype systems for breast cancer detection, all generally based on measuring the time between the transmitted signal and the return of the large reflection from the skin; The Impulse Response (IR) algorithm improves the accuracy of the skin location compared to a simple Peak Detection (PD) algorithm [11]. Although the IR approach has been evaluated successfully using numerical and MRI-derived data in [12, 13], there is a need for validating this method in realistic environments considering non-homogeneous breast phantoms with dispersive skin materials. The method of tangents accurately approximates the breast surface in numerical scenarios assuming that the antenna elements are closely spaced relative to the breast curvature [14]. However, for the array configuration considered herein [7, 8], this assumption is violated and the method cannot accurately estimate the breast surface.

The breast surface identification (BSID) algorithm proposed in [15] initially reconstructs M of breast surface points from M measured data sets. Then interpolation and extrapolation procedures are applied to these M points to generate $N > M$ points that are uniformly distributed over the complete breast surface [15]. The BSID approach gives good results for various realistic breast phantoms however in [15] the authors note that there is scope for improved accuracy; the present contribution presents a very different but complementary surface identification approach. The laser sensor used for estimating the breast skin position results in a fast and accurate reconstruction of the breast surface for both radar-based [16] and tomographic prototype systems [17]. However, for a fully populated array design (e.g. [7, 8]) incorporation of a laser is problematic and indeed costly. The Inverse Boundary Scattering Transform (IBST) was proposed in [18] for planar breast surface reconstruction. However, the use of the signal derivative in the IBST calculation can result in poor resolution reconstruction at high noise levels [18].

In [19], a novel breast surface reconstruction algorithm was proposed for application to the 31-element array. The presented method is based on the Envelope algorithm originally proposed by Kidner *et al.* in [20]. The Envelope algorithm was selected for breast surface reconstruction over the approaches considered in [11-18] since it offers high-accuracy surface reconstructions of arbitrary-shaped targets in scenarios considering various noise levels [20, 21]. In [22], the 2-D Envelope algorithm initially proposed in [19] for the purpose of 2-D breast surface estimation was extended to 3-D using bistatic data for the first time. In [22], this extended Envelope algorithm was evaluated using numerical data. From this prior work in [19, 22], it was concluded that the extended

Envelope algorithm was suitable for use by the 60-element array in recent clinical trials.

There are three distinct differences in the work proposed in the present contribution compared to [19, 22]. First, this paper addresses the application of the extended Envelope algorithm using the geometry and configuration of a 60-element array proposed in [7,8]. Second, this algorithm is further modified in order to manipulate data extracted from phantom measurements and volunteer scans prior to its application at a clinical set up. Thirdly, the method is compared herein with an alternative qualitative approach based on measuring the similarity of the early-time signal contributions of the radar signals. In the clinical setting, a reliable solution to the breast fitting problem might require a rapid qualitative measure followed by a more detailed quantitative measure. The motivation behind the development of the two proposed approaches stemmed from this notion. In this paper, for the first time, the two proposed approaches are evaluated using data extracted from breast phantom measurements and data obtained from scanning human subjects.

The proposed approaches are intended to identify the location of any badly-fitted breast area based on breast surface identification and allow the system user to re-position the patient's breast in the cup/insert accordingly. Once a good fit of the patient's breast is obtained, the breast is re-scanned. Then the array is rotated and the breast is scanned again. The two data sets may then be subtracted with confidence and finally focused.

The proposed approaches altogether take less than 12 seconds of real-time data processing, which is fast given that the data acquisition takes approximately 25 seconds. Once a badly-fitted breast outcome is obtained the patient's breast is re-positioned. The process of obtaining a good fit is patient-specific and thus can take from 60 seconds to several minutes.

This contribution primarily focuses on the application of these algorithms to a hemispherical array. However, it will be appreciated that both the approaches are to a large extent applicable to microwave imaging systems for breast cancer detection (or any such similar problem) with different array configuration (e.g. cylindrical) using monostatic or bistatic radar data. These imaging systems may require a degree of surface identification either for breast fitting information as discussed in this work; for skin reflection reduction (before image focusing [23]) or in microwave tomography (i.e. for use as a priori information in the reconstruction [24]).

This contribution is organised as follows; Section II provides a short description of the improvements introduced to the extended Envelope algorithm for the manipulation of measured data. In Section III, the proposed approach for the qualitative measure of the breast fitting is described. In Section IV, the two proposed approaches are validated using data from phantom measurements and from scanning human subjects. Conclusions are drawn in Section V.

II. QUANTITATIVE BREAST SURFACE IDENTIFICATION APPROACH BASED ON THE EXTENDED ENVELOPE ALGORITHM

The process of estimating the breast surface consists of two distinct steps; the correlation step and the surface reconstruction step as described in [22]. In a clinical setting,

the set of template signals used in the correlation step is produced by a radar measurement of a water-filled cup. The water-cup interface provides a consistent and strong reflection that approximates the skin reflected signal if the breast was perfectly fitted to the shells/cup (since various ceramic inserts are used, water measurements are taken with every insert). In addition, a measurement of the ceramic cup filled with matching medium is used to calibrate-out the direct signal component travelling from the transmitting antenna to the receiving antenna in a straight line path. Since the matching medium and the ceramic cup/ inserts are assumed to have the same relative permittivity in the frequency range of interest, the reflections from this interface will be very small.

Prior to the correlation, both the received and template signals are windowed, where the window length is calculated based on the signal path from the transmitting antenna, to the point of reflection (assuming perfect fitting of the breast in the cup/ inserts) and back to the receiving antenna considering the permittivity of the matching medium/ceramic cup.

For each bistatic observation, the propagation distance values are calculated from the round trip delay values (computed from the correlation function) and fed to the surface reconstruction function. By extending the surface reconstruction function described in [22] to consider the bistatic mode, every propagation distance value will yield a 3-D ellipsoid with the transmitting and receiving antenna positions as its foci. The breast surface points are then found from the intersection of the ellipsoids with a line defined by the centre of the array (origin) and the radius of the cup/insert used. Similarly to [22], the boundary point of the breast is chosen to be the intersection closest to the origin. From a physical point of view, the line corresponds to the radius of the breast as limited by the selected points of the various ellipsoids.

In the experimental system, the radar signals include reflections from cabling and within the array structure, the tumour response and reflections due to the heterogeneity of the breast tissues. As a result, the correlated signal can have several equally-high peaks. For this reason, an additional processing step is introduced to the extended Envelope algorithm compared to [19, 22]. For every (θ, φ) , the two closest reconstruction points - obtained from different ellipsoids - to the origin are averaged to improve the breast surface reconstruction quality.

In the case of the 60-element array, from all the measured bistatic paths (of which are 1770), 101 bistatic paths were selected for the surface reconstruction. As a general rule, the bistatic observations used by the extended Envelope algorithm are selected based on the condition that the distance between the corresponding transmitting and receiving antennas should be less than the distance corresponding to the signal travelling from the transmitter, impinging at the point of reflection (i.e. the surface of the breast) and recorded at the receiver, for the case of specular reflection assuming a perfectly-fitted breast.

From the reconstructed breast surface, an error value is calculated (in mm) using the following equation:

$$error(\theta, \varphi) = r_{cup} - \sqrt{(x(\theta, \varphi) - x_0)^2 + (y(\theta, \varphi) - y_0)^2 + (z(\theta, \varphi) - z_0)^2} \quad (1)$$

where r_{cup} represents the radius of a ceramic insert used, (x_0, y_0, z_0) denotes the centre of the antenna array and $(x(\theta, \varphi), y(\theta, \varphi), z(\theta, \varphi))$ refer to every (θ, φ) reconstructed point. These error values are illustrated in a 2-D projection of the cup (as shown in Fig. 3-(a), 5-(a), 7-(a) to 11-(a)).

The extended Envelope algorithm will result in $151 \times 152 = 22952$ reconstruction points that will correspond to a reconstruction resolution for the 2-D projection map equal to approximately 2.4mm.

III. QUALITATIVE BREAST SURFACE IDENTIFICATION APPROACH

The alternative, qualitative method presented in this section is largely based on the similarity of grouped bistatic signals using Pearson correlation coefficient calculation. The correlation coefficient has been used in the literature for data processing [25, 26], image processing [27, 28] and biomedical applications [29]. In [29], the correlation coefficient is used to measure the gait signal similarity in order to classify healthy people from hemiplegics. In this contribution, the correlation coefficient is used, for the first time, as a measure of signal similarity for the purpose of qualitative surface identification in the context of microwave breast imaging. The proposed approach is as follows: initially, the windowed early-time signal contributions (skin reflections) of the calibrated time-domain radar signals are considered as described in Section II. The signals are then grouped together into sets of four signals based on groups of symmetrically-distributed antenna pairs within the array. For instance, from Fig. 1, a group of bistatic signals would correspond to antenna pairs: 29-38, 38-46, 38-47 and 30-38.

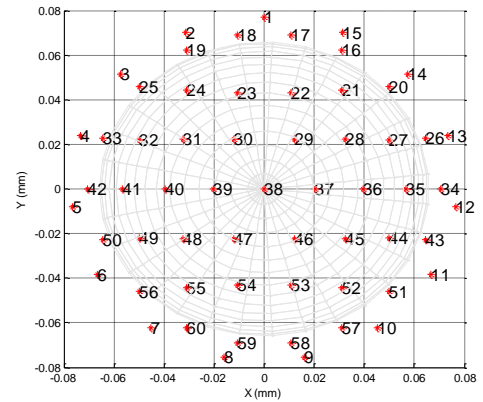


Fig. 1 2-D schematic of the 60-element antenna array

For a group of signals, a reference signal $F(t)$ is defined using the following equation:

$$F(t) = \frac{\hat{y}_1(t) + \hat{y}_2(t) + \hat{y}_3(t) + \hat{y}_4(t)}{4} \quad (2)$$

where $\hat{y}_1(t)$, $\hat{y}_2(t)$, $\hat{y}_3(t)$ and $\hat{y}_4(t)$ are the four windowed signals of the group. For the i^{th} signal of the group, the similarity coefficient r_i , which is effectively the correlation coefficient, is expressed by the following equation:

$$r_i = \frac{\text{cov}(F, \hat{y}_i)}{\sigma_F \sigma_{y_i}} \quad (3)$$

where the numerator refers to the covariance matrix between the reference signal $F(t)$ and each windowed signal $\hat{y}_i(t)$ and σ_F σ_{y_i} are the standard deviations for the signals $F(t)$ and $\hat{y}_i(t)$ respectively. For ease of visualisation, the similarity coefficient r_i corresponding to the i -th bistatic observation is positioned at the mid-point of the respective transmitting and receiving antenna pair (as depicted in Fig. 3-(b), 5-(b), 7-(b) to 11-(b)). A correlation coefficient value approximating 0 corresponds to a bad fitting and 1 corresponds to a good fitting. For this approach, the visualisation map yields a qualitative measure of the fitting corresponding to a spatial resolution equal to approximately 15mm.

IV. ANALYSIS OF RESULTS

A. Methods validation considering phantom measurements

Initially, a set of phantom measurements were performed in order to validate the performance of the two proposed fitting measuring approaches.

1. Perfectly fitted breast phantom

First, the scenario representing a perfectly fitted breast in the ceramic cup was considered. A 2mm-thick skin phantom ($\epsilon_r=35$ at 6GHz [10]) was placed in the ceramic cup, with just a small amount of matching medium between the skin layer and the cup, to ensure good contact. Fig. 2 shows the skin layer in the cup. The cup was then filled with matching medium representing the internal breast tissues. The outputs for the proposed breast fitting measuring approaches are shown in Fig. 3-(a) and (b).

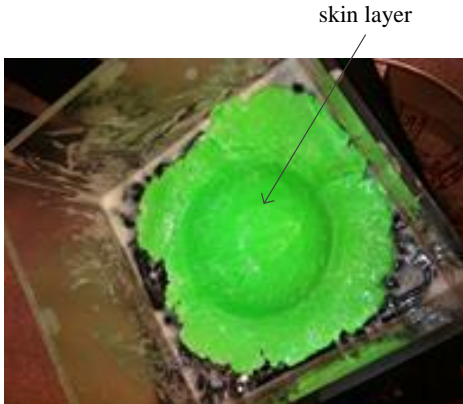


Fig. 2 Skin layer material fitted in the ceramic cup

It can be observed from Fig. 3-(a) that the breast phantom is well fitted in the ceramic cup with a mean error equal to approximately 2mm. This error is within the experimental tolerances of the phantom construction. In Fig. 3-(b), the majority of the similarity coefficients are close to unity, showing the good fitting of the phantom in the cup. There is good agreement between the two approaches in this case.

It can be observed from Fig. 3-(a) that there is an area in the centre of the cup which indicates a gap in the range of approximately 3mm. The matching liquid tends to flow

towards the centre of the cup's curvature, pushing the skin layer away from the cup. Due to the error's symmetry, the groups of signals corresponding to antenna pairs located underneath this part of the skin phantom have similar early-time contributions. Thus, the output of the proposed method based on the early-time signal similarity (shown in Fig. 3-(b)) is unable to identify this particular fitting error.

Around the very outer periphery in Fig. 3-(a) it can be noted that the algorithm does not work correctly in reconstructing the breast surface at the top of the breast close to the chest wall, largely due to the limited number of antennas that can observe signals from that region.

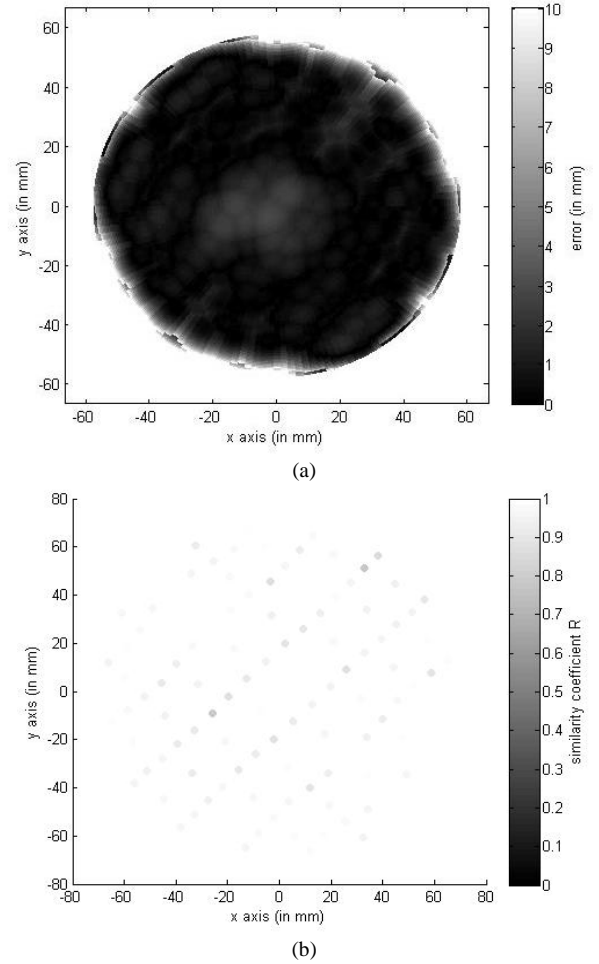


Fig. 3 Measuring fitting for perfectly fitted breast phantom: (a) quantitative breast surface reconstruction, (b) qualitative similarity of the skin reflection signal contributions

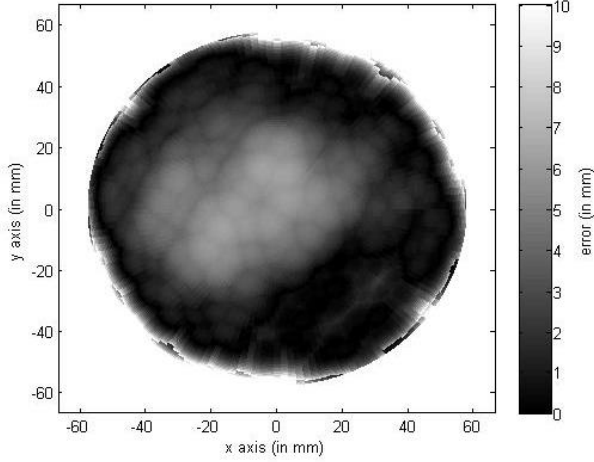
2. 6mm matching medium gap phantom

In the second experimental scenario, a piece of cardboard was rolled in the shape of a circle with a thickness equal to approximately 6mm and then soaked in matching medium liquid to acquire its dielectric properties. This was placed in the ceramic cup (Fig. 4) and then the skin phantom was placed on top, thereby creating a 6mm-thick gap in the centre of the ceramic cup. Finally, matching medium filled the cup. This scenario is intended to represent a badly fitted breast. Fig. 5-(a) and (b) depict the outputs of the two proposed fitting

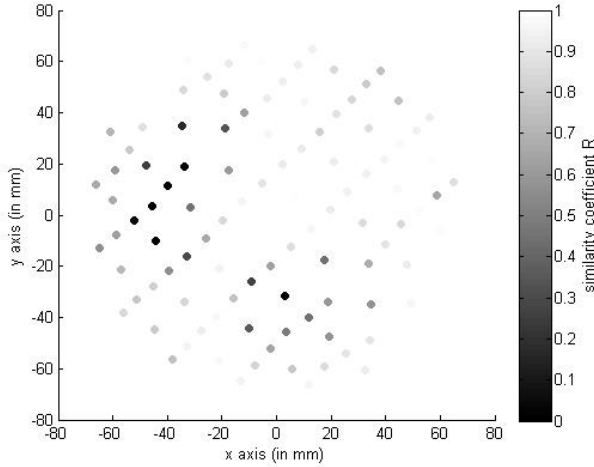
measuring approaches.



Fig. 4 Piece of cardboard to create the gap



(a)



(b)

Fig. 5 Measuring fitting for 6mm liquid gap phantom: (a) quantitative breast surface reconstruction, (b) qualitative similarity of the skin reflection signal contributions

It can be observed from Fig. 5-(a) that the extended Envelope algorithm can accurately identify the location of the gap. The region containing matching medium is not entirely symmetric and covers a large area of the cup's curvature. The lack of symmetry could be due to the fact that the amount of matching medium liquid is large, shifting the cardboard in one direction. Since the majority of the groups of symmetrically positioned antenna pairs are located underneath the centrally matching-medium-filled area, the early-time contributions of the corresponding bistatic signals are similar. As a result, the

qualitative technique again cannot identify this area, as shown in Fig. 5-(b). As observed in Fig. 5-(a) and (b), the asymmetric error for x and y in the range $[-40, -20]$ and $[-20, 20]$ mm respectively is identified by both fitting measuring approaches.

3. Phantom with small air gap at 3 o'clock

In this scenario, an approximately 3mm-thick air gap was introduced to the breast surface placed approximately 3 o'clock in the ceramic cup. The air gap was created by a piece of bubble wrap inserted in the cup prior to placing the skin phantom. For the bubble wrap, the thickness of the plastic is less than 0.5mm. Therefore, it is assumed that a radar signal meets first the matching medium/air interface. Fig 6 depicts the bubble wrap inserted in the ceramic cup. Fig. 7-(a) and (b) demonstrate the outputs of the proposed fitting measuring approaches.

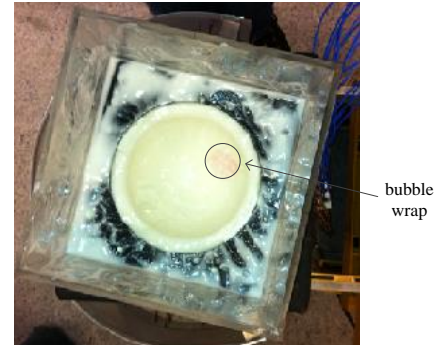
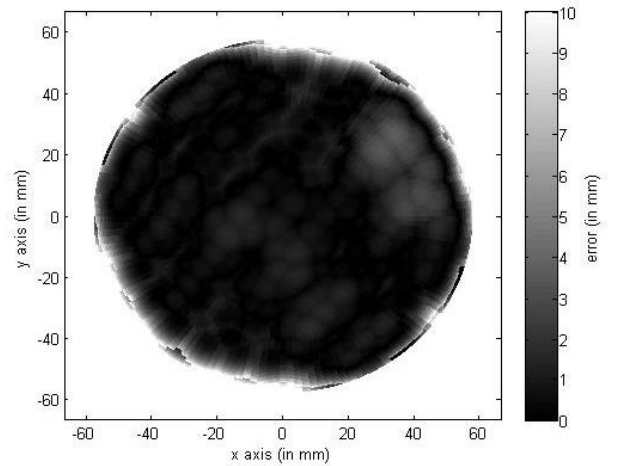


Fig. 6 Phantom with small airgap at 3 o'clock

It can be observed from Fig. 7-(a) that the location of the gap is accurately detected by the extended Envelope algorithm. The proposed approach for qualitative measure of the breast fitting also correctly identifies the position of the gap as shown in Fig. 7-(b).



(a)

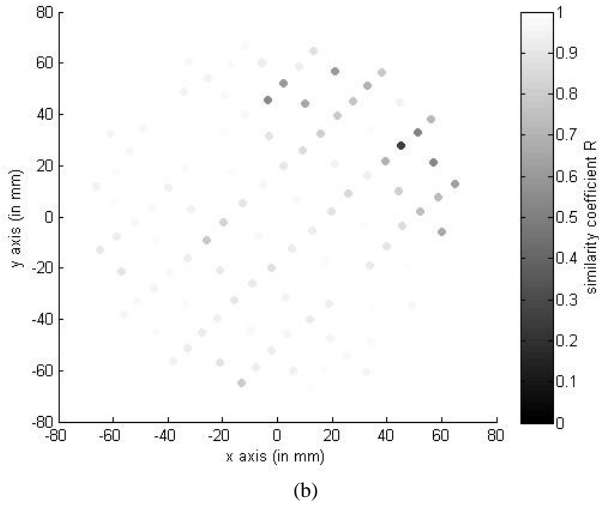


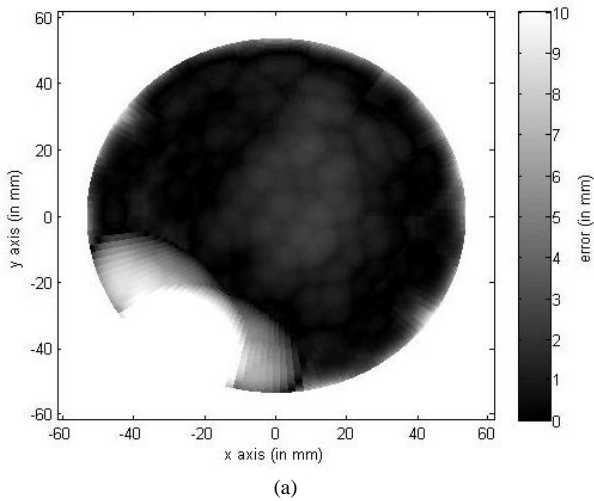
Fig. 7 Measuring fitting for phantom with small airgap at 9 o'clock: (a) quantitative breast surface reconstruction, (b) qualitative similarity of the skin reflection signal contributions

B. Method application to volunteer data

In addition to the phantom experiments, a female volunteer was scanned in order to further assess the effectiveness of the proposed approaches prior to their use in the clinic. Several scenarios were considered to emulate realistic situations that arise in a clinical setting.

1. Volunteer badly fitted in cup

Initially, an amount of matching medium liquid was placed in the cup and then the volunteer's breast was positioned in the ceramic cup. Without trying to ensure a good fit, the breast was scanned using the radar system. The outputs of the proposed fitting measuring approaches are provided in Fig. 8-(a) and (b).



(a)

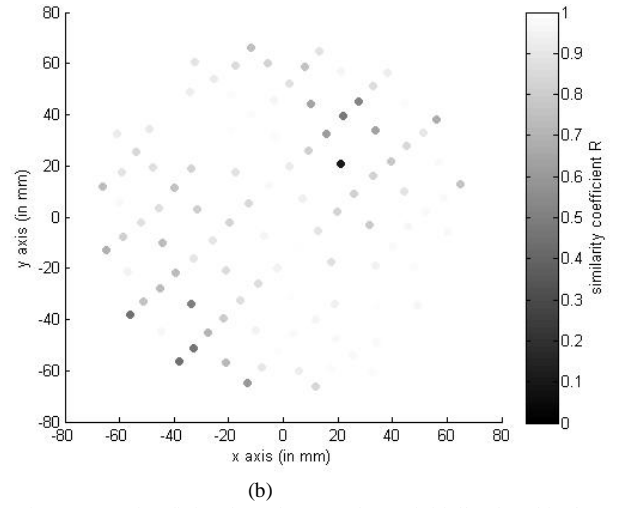
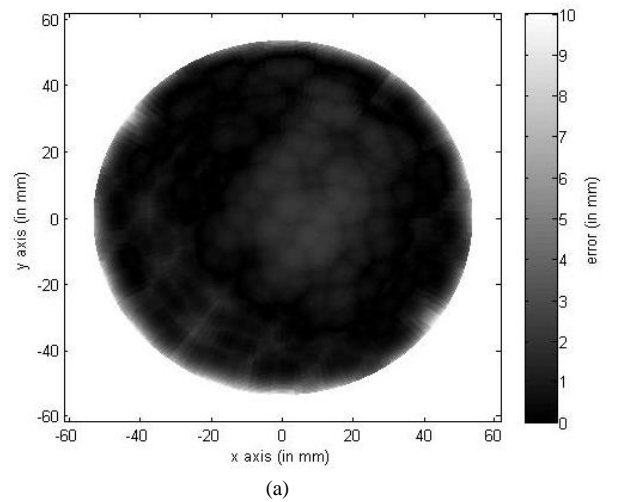


Fig. 8 Measuring fitting for volunteer's breast initially placed in the cup (a) quantitative breast surface reconstruction, (b) qualitative similarity of the skin reflection signal contributions

It can be observed from Fig. 8-(a) that the main breast volume is well fitted in the cup ensuring a mean error equal to approximately 2mm. A fitting error greater than 4mm at the part of the breast close to 7 o'clock in the figure is observed. This area of bad fitting is also identified in the qualitative approach (seen in Fig. 8-(b)). The poor fitting probably comprises an air gap, which is likely to occur at the edges of the ceramic cup. Since for the extended Envelope algorithm, the round trip propagation distance calculations assume the relative permittivity value of the matching medium rather than that of the air, this output probably over-estimates the degree of bad fitting.

Based on the data shown in Fig. 8, the patient's breast was rearranged in the cup (this can be achieved by lowering the trolley on top of which the system is placed and lifting it up again). The volunteer's breast was then scanned again and the outputs of the two approaches are illustrated in Fig. 9-(a) and (b).



(a)

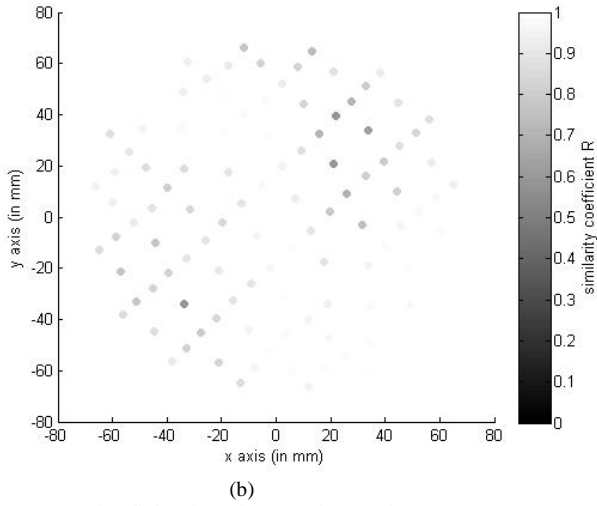


Fig. 9 Measuring fitting for volunteer's breast after re-fitting (a) quantitative breast surface reconstruction, (b) qualitative similarity of the skin reflection signal contributions

By visually comparing Fig. 8-(a) and 9-(a) it can be seen that the breast re-arrangement has resulted in a significantly improved fit. Similarly, from the comparison of Fig. 8-(b) and 9-(b) it can be observed that the main area of bad fitting is eliminated.

The approximately 3mm fitting error located approximately at the centre of the cup in both Fig. 8-(a) and 9-(a) is attributed to the nipple. This error is better illustrated by the qualitative approach as depicted in Fig. 8-(b) and 9-(b). Due to its structure, the nipple is not fitted perfectly in the ceramic cup, 'pushing' the surrounding breast area away from cup. This fitting error is identified by the second approach as shown in Fig. 9-(b).

2. Patch of air located at the centre of the cup

In this scenario, a piece of bubble wrap of thickness equal to approximately 3mm was inserted approximately at the centre of the cup. Then the volunteer's breast was fitted in the cup. Fig. 10-(a) and (b) depict the degree of fitting of the breast in the ceramic cup.

It can be observed from Fig. 10-(a) and (b) that the location of the air gap is accurately detected from both proposed fitting measuring approaches. The fitting error is measured by the extended Envelope algorithm approximately equal to 4mm as shown in Fig. 10-(a). This over-estimation is probably caused by the assumption made about the velocity of propagation as mentioned previously.

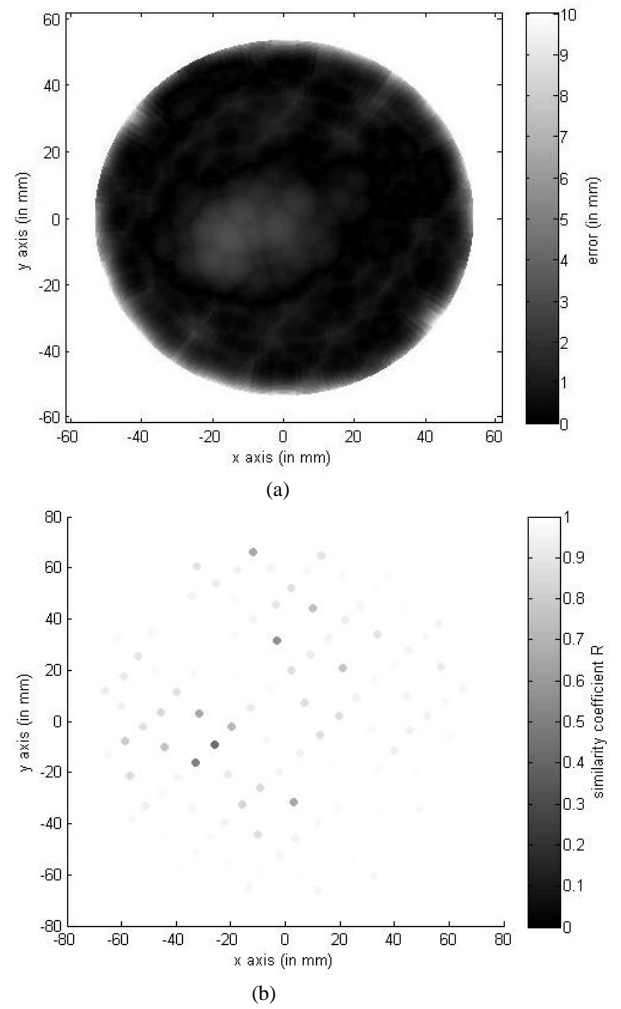


Fig. 10 Measuring fitting for volunteer's breast with a patch of air located at the centre of the cup: (a) quantitative breast surface reconstruction, (b) qualitative similarity of the skin reflection signal contributions

3. Patch of air located at 9 o'clock

In this test case, the piece of bubble wrap used in the previous scenario was placed in the cup approximately at 9 o'clock. Fig. 11-(a) and (b) demonstrate the outputs of the proposed fitting measuring approaches.

The output shown in Fig. 11-(a) identifies accurately the location of the fitting error over-estimating its magnitude due to the mechanics of the breast surface reconstruction algorithm. The low correlation coefficient values for the antenna pairs located approximately at 9 o'clock verify the presence of the bad fit in the output depicted in Fig. 11-(b).

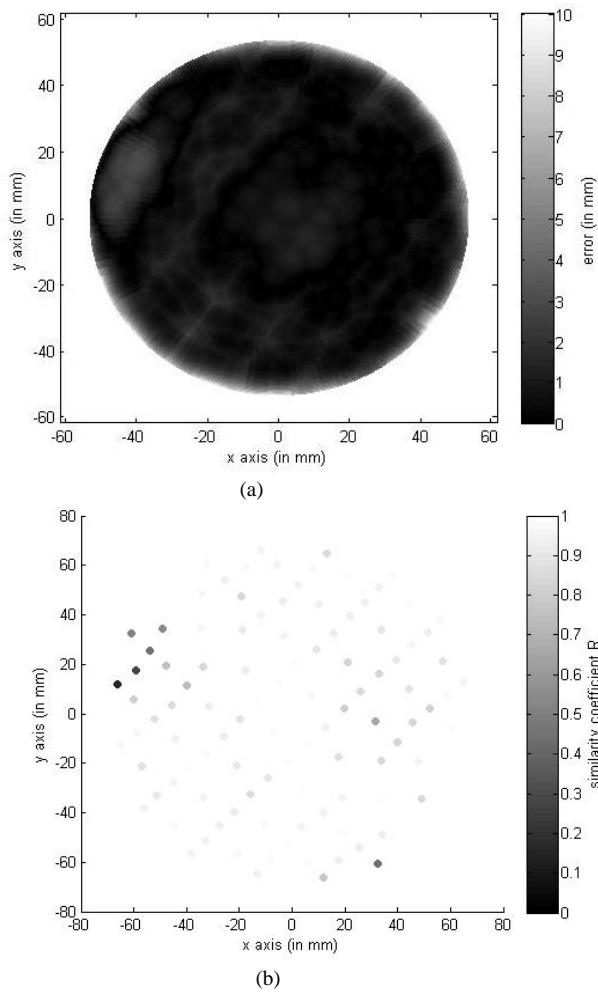


Fig.11 Measuring fitting for volunteer's breast with a patch of air located at 3 o'clock: (a) quantitative breast surface reconstruction, (b) qualitative similarity of the skin reflection signal contributions

V. CONCLUSION

The proposed approaches are implemented to a 60-element hemispherical array used in clinical trials currently conducted at Southmead Hospital, Bristol, UK. The first approach aims at giving a quantitative measure of the breast fitting in the ceramic cup/inserts by reconstructing the breast surface. The second approach is based on the similarity of the early-time signal contributions for the radar signals of symmetrically located antenna pairs. The two approaches complement one another in order to enhance the fitting process during the clinical trial.

The effectiveness of the proposed signal processing approaches was evaluated using phantom and volunteer data. It was concluded that they can provide significant assistance by giving both qualitative and quantitative measures of the fitting of the patient's breast to the ceramic cup/ inserts. The extended Envelope algorithm can measure the thickness of a matching medium gap within 1mm accuracy. However, this algorithm cannot differentiate between an air and a matching medium gap. The proposed approach based on the signal similarity identifies fitting errors accurately complementing the observation of the extended Envelope algorithm, but also cannot visualise the difference between air and matching medium gaps. By comparing the proposed approaches, it can

be concluded that the extended Envelope algorithm is more sensitive to the presence of a gap (e.g. fluid or air) in any area of the cup. Conversely, the proposed qualitative method based on signal similarity cannot detect gaps located in the centre of the cup/insert.

As explained herein, the proposed approaches for surface localisation are applicable to any similar such imaging system; either for fitting or for actual imaging. In addition, the proposed approaches have low computational cost and therefore, as here, can assist the operator in real time during the patient imaging procedure.

REFERENCES

- [1] "Mammography and Beyond: Developing technologies for early detection of breast cancer", Washington DC: Institute of Medicine, National Academy of Sciences Press, 2001.
- [2] Cancer Research UK (available online at: <http://info.cancerresearchuk.org/>).
- [3] P. T. Huynh, A. M. Jarolimek, S. Daye, "The false-negative mammogram", *RadioGraphics*, vol. 18, no. 5, pp. 1137-1154, 1998.
- [4] E. C. Fear, P. M. Meaney and M. A. Stuchly, "Microwaves for breast cancer detection?", *IEEE Potentials*, vol. 22, issue 1, pp. 12-18, 2003.
- [5] E. C. Fear, S. C. Hagness, P. M. Meaney, M. Okoniewski, M. A. Stuchly, "Enhancing breast tumor detection with near-field Imaging", *IEEE Microwave magazine*, vol. 3, issue 1, pp. 48-56, March 2005.
- [6] M. Klemm, J.A. Leendertz, D. Gibbins, I.J. Craddock, A. Preece, M. Shere and R. Benjamin, "Clinical trials of a UWB imaging radar for breast cancer", *European Conference on Antennas and Propagation (EuCAP)*, pp. 1-4, Spain 2010.
- [7] M. Klemm, D. Gibbins, J.A. Leendertz, T. Horseman, A. Preece, R. Benjamin, I.J. Craddock, "Development and testing of a 60-element UWB conformal array for breast cancer imaging", *European Conference on Antennas and Propagation (EuCAP)*, pp. 1-4, 2011.
- [8] T. Henriksson, M. Klemm, D. Gibbins, T. Horseman, A. W. Preece, R. Benjamin and I.J. Craddock, "Clinical trials of a multistatic UWB radar for breast imaging", *Loughborough Antennas and Propagation Conference (LAPC)*, pp. 1-4, 2011.
- [9] M. Klemm, I.J. Craddock, J.A. Leendertz, A.W. Preece and R. Benjamin, "Radar-based breast cancer detection using a hemispherical antenna array- experimental results", *IEEE Transactions on Antennas and Propagation*, vol. 57, no. 6, pp. 1692-1704, June 2009.
- [10] M. Klemm, J.A. Leendertz, D. Gibbins, I.J. Craddock, A.W. Preece and R. Benjamin, "Microwave radar-based differential breast cancer imaging: imaging in homogeneous breast phantoms and low contrast scenarios", *IEEE Transactions on Antennas and Propagation*, vol. 58, no. 7, pp. 2337-2344, July 2010.
- [11] T. W. Williams, J. M. Sill and E. C. Fear, "Robust Approach to Skin Location Estimation for Radar-Based Breast Imaging Systems", *IEEE EMBS Conference*, Vancouver, British Columbia, Canada, pp. 5837-5841, 2008.
- [12] T. C. Williams, E. C. Fear and D. T. Westwick, "Tissue Sensing Adaptive Radar for Breast Cancer Detection- Investigations of an Improved Skin-Sensing Method", *IEEE Transactions on Microwave Theory and Techniques*, vol. 54, no. 4, pp. 1308-1314, 2006.
- [13] T. C. Williams, J. M. Sill and E.C. Fear, "Breast surface estimation for radar-based breast imaging systems", *IEEE Transaction on Biomedical Engineering*, vol. 55, no. 6, pp. 1678-1686, June 2008.
- [14] X. Li, E. J. Bond, B. D. Van Veen and S. C. Hagness, "An Overview of the Ultra-Wideband Microwave Imaging via Space-Time Beamforming for Early-Stage Breast-Cancer Detection", *IEEE Antennas and Propagation Magazine*, vol. 47, no. 1, pp. 19-34, 2005.
- [15] D. W. Winters, J. D. Shea, E. L. Madsen, G. R. Frank, B. D. Van Veen and S. C. Hagness, "Estimating the Breast Surface Using UWB Microwave Monostatic Backscatter Measurements", *IEEE Trans. Biomed. Eng.*, Vol. 55, no. 1, pp. 247-255, 2008.
- [16] T. C. Williams, J. Bourqui, T.R. Cameron, M. Okoniewski, E.C. Fear, "Laser surface estimation for microwave breast imaging systems", *IEEE Transactions on Biomedical Engineering*, vol. 58, no. 5, pp. 1193-1199, May 2011.

- [17] M. J. Pallone, P. M. Meaney and K. D. Paulsen, "Surface scanning through a cylindrical tank of coupling fluid for clinical microwave breast imaging exams", *Med. Phys.* pp. 3102-3111, 39 (6), June 2012.
- [18] M. Helbig, M. A. Hein, U. Schwarz, J. Sachs, "Preliminary investigations of chest surface identification algorithms for breast cancer detection", *IEEE International Conference on Ultra-Wideband (ICUWB)*, vol. 2, pp. 195-198, 2008.
- [19] M. Sarafianou, D. R. Gibbins, I. J. Craddock, M. Klemm, J. A. Leendertz, A. Preece, R. Benjamin, "Breast surface reconstruction algorithm for a multi-static radar-based breast imaging system", *4th European Conference on Antennas and Propagation (EuCAP)*, pp. 1-5, 2010.
- [20] S. Kidera, T. Sakamoto and T. Sato, "A robust and fast imaging algorithm with an envelope of circles for UWB pulse radars", *IEICE Trans. Commun.*, vol. E90-B, no. 7, pp. 1801-1809, 2007.
- [21] S. Kidera, T. Sakamoto and T. Sato, "High-Resolution and Real-Time Three-Dimensional Imaging Algorithm With Envelopes of Spheres for UWB Radars", *IEEE Trans. on Geoscience and Remote Sensing*, vol. 46, no. 11, pp. 3503-3513, 2008.
- [22] M. Sarafianou, D. R. Gibbins, I. J. Craddock, "A novel 3-D breast surface reconstruction algorithm for a multi-static radar-based breast imaging system", *Proceedings on Loughborough Antennas and Propagation Conference (LAPC) 2011*.
- [23] M. Sarafianou, I. J. Craddock and T. Henriksson, "Towards Enhancing Skin Reflection Removal and Image Focusing Using a 3-D Breast Surface Reconstruction Algorithm". *IEEE Transactions on Antennas and Propagation*, vol 61, pp. 5343-5346, 2013.
- [24] J. E. Johnson, T. Takenaka and T. Tanaka, "Two-dimensional time-domain inverse scattering for quantitative analysis of breast composition", *IEEE Transactions on Biomedical Engineering*, vol. 55, no. 8, pp. 1941-1945, 2008.
- [25] K. B. Logoglu, T. K. Ates, "Speeding-up Pearson correlation coefficient calculation on graphical processing units", *IEEE 18th Signal Processing and Communications Applications Conference*, pp. 840-843, 2010.
- [26] K. Kipli, S. Krishnan, N. Zamhari, M. S. Muhammad, S. M. W. Masra, C. Lee Kho, K. Lias, "Full reference image quality metrics and their performance", *IEEE 7th International Colloquium on Signal Processing and Applications (CSPA)*, pp. 33-38, 2011.
- [27] W. P. Marshak, D. J. Darkow, "Objective measurement of display formats: multidimensional and multimodel user perception", *International Conference on Image Processing (ICIP)*, vol. 2, pp. 505-509, 1998.
- [28] M. Vranjes, S. Rimac-Drije, K. Grgic, "Locally averaged PSNR as a simple objective video quality metric", *50th International Symposium ELMAR*, vol. 1, pp. 17-20, 2008.
- [29] M. Djuric-Jovicic, I. P. Milovanovic, N. S. Jovicic, D. B. Popovic, "Reproducibility of "BUDA" multisensor system for gait analysis", *IEEE EUROCON*, pp. 108-111, 2008.